

Highly Conductive Ionic Liquids toward High-Performance Space-Lubricating Greases

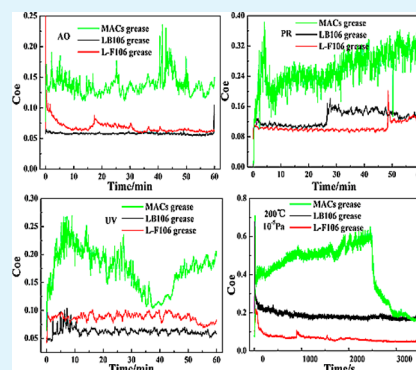
Xiaoqiang Fan^{†,‡} and Liping Wang^{*,†}

[†]State Key Laboratory of Solid Lubrication, Lanzhou Institute of Chemical Physics, Chinese Academy of Sciences, Lanzhou 730000, P.R. China

[‡]University of Chinese Academy of Sciences, Beijing 100039, P.R. China

ABSTRACT: Although ionic liquids (ILs) as a class of promising materials have a wide range of applications due to the excellent properties, their potential as space lubricants has been not systematically explored. Here two kinds of conductive alkyl imidazolium ILs greases were prepared using 1-hexyl-3-methylimidazolium tetrafluoroborate (LB106) and 1-hexyl-3-methylimidazolium bis-(trifluoromethylsulfonyl) amide (L-F106) as base oil and the polytetrafluoroethylene (PTFE) as thickener, with multiple-alkylated cyclopentane grease (MACs) as a comparison. Their chemical composition and tribological properties were investigated in detail under simulated space environment which is composed of high vacuum, high temperature and irradiation. Results show that the high conductive ILs greases not only possess good adaptive abilities to space environment and thermal stability but also provide excellent friction reducing and antiwear behaviors as well as high load carrying capacities. The unique physicochemical properties are attributed to a combination of special anions and cations, the excellent tribological properties are strongly dependent on a boundary protective film on the rubbing surfaces.

KEYWORDS: ionic liquids, vacuum, space irradiation, conductivity, tribochemistry



1. INTRODUCTION

Artificial satellites and spacecrafts in low earth orbit or inner space were installed with various drive mechanisms.¹ Their reliability and accuracy are vitally important because the breakdown of these elements can easily inflict fatal damage to the satellites and spacecrafts with no possibility of repair.^{2,3} With the continuous improvement of machine elements over the past few decades, the challenges of lubrication issues have impeded the human exploration of the universe.^{4,5} The increasing growth in the field of space technology has also urgently required the intense development of lubricants. Although a large number of attempts have been successfully made to introduce some lubricating materials to space environment,^{6,7} they can not fulfill the continuous developing demands of space technology.

It is very significant and valuable to research on the physicochemical properties and friction behaviors of lubricants under simulated space conditions because these properties are closely associated with low friction and wear, low mechanical noise and adaptive capacity to space environment.^{8,9} The space environment differs greatly from atmospheric environment, which includes high vacuum (HV), high/low temperature, ultraviolet irradiation (UV), atomic oxygen (AO), proton irradiation (PR), and so on.^{10–12} For instance, under space environment, evaporation loss of lubricants must be considered with regard to the lubrication problems. Besides, temperature can change from -120 to 150 °C because of the influence of sunlight, so lubricants must possess a wide temperature range

for space application. Moreover, since energetic atomic oxygen and proton could interact with materials and change the molecules structure of materials, lubricants need to enhance anti-irradiation performance.^{13–15}

In view of harsh space environment, our attention has been focused on the versatile ionic liquids (ILs) that are composed of a relatively large organic cation and a weakly coordinating inorganic anion.¹⁶ ILs have been widely studied as lubricant and candidate to substitute traditional volatile organic solvents due to their unique properties such as negligible vapor pressure, excellent thermal stability, wide temperature range, high electrical conductivity and good tribological properties.^{17–19} Although ILs have been investigated as excellent lubricants for contacts of steel/steel, steel/aluminum, steel/copper and modified surface coating/steel,^{20–27} they have not been systematically studied under simulated space environment.

In this paper, great efforts are made to explore the physicochemical properties and space performance of ILs. With multialkylated cyclopentane (MACs) as comparison, which has been widely recognized on actual space hardware, high conductive ILs greases were prepared using 1-hexyl-3-methylimidazolium tetrafluoroborate (LB106) and 1-hexyl-3-methylimidazolium bis(trifluoromethylsulfonyl) amide (L-F106) as base oil and the polytetrafluoroethylene (PTFE) as

Received: June 22, 2014

Accepted: August 4, 2014

Published: August 4, 2014

a thickener. Their composition and physicochemical properties as well as tribological performance before and after irradiation were evaluated in detail.

2. EXPERIMENTAL SECTION

2.1. Materials. According to the literature,^{28–30} two kinds of alkyl imidazolium ILs were prepared, the corresponding chemical formulations of LB106 and L-F106 ILs are shown in Figure 1 and

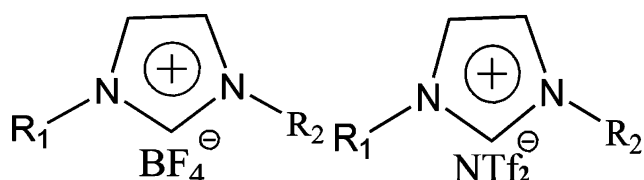


Figure 1. Chemical formulations of LB106 and L-F106 ILs ($R_1 = C_6H_{13}$, $R_2 = CH_3$).

their physical properties (conductivity, viscosity and density) are listed in Table 1. MACs grease was provided by Lanzhou Institute of

Table 1. Physical Properties of Ionic Liquids

code (base oil)	conductivity ($\mu S\ cm^{-1}$)	kinematic viscosity (mm^2/s)		viscosity index	density (g/mL) at 25 °C
		40 °C	100 °C		
L-B106	1193	82.5	11.9	138	1.148
L-F106	1181	66.4	10.0	135	1.207

Chemical Physics, Chinese Academy of Sciences (Lanzhou, China). Acetone and polytetrafluoroethylene (PTFE) micropowder were also commercially obtained. The grain size and density of the PTFE micropowder are about 4 μm (Dyneon, TF9207) and 2.2 g/cm^3 . All chemical reagents were of analytical grade and used without further purification.

2.2. Preparation and Characterization of the ILs-Greases.

The IL-greases were prepared according to the following procedures. 75 wt % neat ILs as base oil was put into the vessel under mild stirring. Then, 25 wt % PTFE as a thickener was slowly added into the vessel under vigorous stirring. When the base oil and the thickener were mixed uniformly, the acetone about half of total mass of the thickener was added dropwise to ensure that the PTFE was completely dispersed throughout the base oil. After continued stirring for about 30 min, the mixture was heated up to 80 °C and maintained at this temperature for about 30 min to remove the acetone. When the mixture had cooled to room temperature, it was introduced to a roller and grinded/homogenized by three close rollers that rotate in opposite directions. Finally, the IL-grease was obtained after three separate fine grinding/homogenization steps in a three-roller mill. The LB106 grease and L-F106 grease were prepared according to the above procedure.

The dropping point and penetration of the lubricating greases were characterized according to the national standards GB/T 3498 and GB/T 269, similar to ASTM D2265 and ASTM D1403, respectively. The copper strip tests of the lubricating greases were performed by the national standards GB/T 7326–87, similar to ASTM D4048–81. The conductivities of the lubricating greases were measured by the DDSJ-308A conductivity meter made by Shanghai INESA & Scientific Instrument CO.Ltd. at 25 °C.

2.3. Irradiation Procedure. AO, UV, and PR irradiation experiments were carried out in ground-based simulation facilities in Lanzhou Institute of Chemical Physics, Chinese Academy of Sciences. The experimental parameters of simulated space irradiation are listed in Table 2. The basic principle schematic illustration of AO irradiation was referred in ref 31. For the space environment, atomic oxygen originates from photodissociation of O_2 in the upper atmosphere, its

Table 2. Experimental Parameters of Space Irradiation

irradiation	parameters	irradiation time (min)	friction testing time (min)
AO	4.6×10^{15} atom/($cm^2\ s$), 5 eV	120	60
PR	500 $\mu A/cm^2$	120	60
UV	800 W/m^2 , 115–400 nm	120	60

number density is about 8×10^7 atoms/ cm^3 at 400 Km altitude, and the AO flux in low earth orbit is 1×10^{14} to 1×10^{15} atoms/ $cm^2\ s$. The solar UV irradiation in the range of 100–400 nm accounts for 8% of the solar wavelength range (0.115 μm up to 50 μm), so the intensity of UV is only about 8% of the total solar energy (1366 W/m^2). The ionizing irradiation includes high energy electrons (up to several MeV), protons (up to several hundred MeV), heavy ions and alpha particles, and proton is the most abundant of ions in high-energy irradiation environment. Energetic proton can cause serious irradiation damage to components and materials. In this paper, the experimental atomic oxygen flux was 4.6×10^{15} atoms/ $cm^2\ s$ with impingement kinetic energy of 5 eV for 120 min at the sample position, the vacuum UV irradiation with energy levels of 800 W/m^2 in the range of 115–400 nm was carried out under high vacuum (1×10^{-5} Pa) for 120 min and the experiment of PR provided the high-intensity beam of protons (500 $\mu A/cm^2$) for 120 min.

2.4. Analysis of the Lubricating Greases before and after Irradiation. To systematically investigate the influence of AO, PR and UV on the lubricating greases, we examined the functional group, decomposition temperature, composition, structure and tribological properties of the lubricating greases before and after irradiation in detail. The functional groups were investigated by Bruker IFS 66v/s Fourier transform infrared analysis (FTIR). Thermogravimetric analysis (TGA) was carried out on a ZRY-2P TGA at a heating rate of 10 °C/min in flowing air. The chemical composition was determined using scanning electron microscopy-energy dispersive X-ray spectroscopy (SEM-EDS) (Oxford IE250 Energy Dispersive Spectrometer, EDS) under 20 kV accelerating voltage with 10 nA beam current. The chemical structure was analyzed by a PHI-5702 multifunctional X-ray photoelectron spectroscope (XPS) made by American Institute of Physics Electronics Company using K-Alpha irradiation as the excitation source. The binding energies of the target elements were determined at a pass energy of 29.3 eV, with a resolution of about ± 0.3 eV, using the binding energy of contaminated carbon (C 1s: 284.8 eV) as the reference.

The friction tests were performed on a self-made rotational ball-on-disk vacuum tribometer under high vacuum. The fixed upper specimens were an AISI 52100 steel ball with standard 6 mm diameter, and the lower specimens were the stainless steel disc. Before friction tests, the irradiated lubricating greases were coated homogeneously on the steel disc. The tests were conducted at rotational radius of 6 mm, sliding speed of 300r/min, applied load of 5N and duration of 60 min at room temperature and under vacuum (1×10^{-5} Pa) condition. The friction behaviors of the lubricating greases at high temperature (200 °C) and under high vacuum (1×10^{-5} Pa) were also investigated. The friction coefficients were monitored continuously as a function of time. Friction test under the same conditions was repeated three times in order to check the reproducibility of the measurements. In addition, the extreme pressure properties of the lubricating greases at high temperature (150 °C) were performed on an Optimal-SRV-IV reciprocation friction tester with a ball-on-block configuration. The upper ball (diameter of 10 mm, AISI 52100 steel, hardness 710HV) slides reciprocally at an amplitude of 1 mm against the stationary lower steel disks (AISI 52100 steel, $\Phi 24 \times 7.9$ mm with hardness of about 618HV). All the tests were set at a load ramp test from 100 to 800N stepped by 50N and the test duration for each load was 5 min. About 1g grease was introduced to the ball-disc contact area and the friction coefficient was recorded automatically by a computer connected to the Optimal-SRV-IV tester. The wear losses of the lower disks were measured using a MicroXAM-3D surface mapping microscope profilometer.

The morphologies of the wear surfaces and the binding energies of some typical elements on the worn surfaces were analyzed by JEM-5600LV scanning electron microscope (SEM) (JEOL, Japan) and PHI-5702 multifunctional X-ray photoelectron spectroscope (XPS), respectively. Prior to testing, the specimens were cleaned ultrasonically several times in baths of acetone and dried with pure nitrogen for surface analysis.

3. RESULTS AND DISCUSSION

3.1. Physical Properties of Lubricating Greases. The physical properties of the lubricating greases are outlined in

Table 3. Physical Properties of the Prepared Lubricating Greases

sample (grease)	dropping point (°C)	penetration (1/4 mm)	copper corrosion (T2 copper, 100 °C, 24 h)	conductivity ($\mu\text{S cm}^{-1}$)
L-B106 grease	243	74	1a	1122
L-F106 grease	224	78	1a	1086

Table 3. The ILs greases have high dropping point (>220 °C) and corrosion resistance property (copper corrosion 1a) as well as higher conductivities (>1000 $\mu\text{S}\cdot\text{cm}^{-1}$) than the traditional conductive lubricating greases which contains conductive filler.^{32,33} The conductivities of the ILs greases originate from the specific cations and anions as well as their strong intrinsic electrostatic interactions. ILs entirely composed of ions exist

strong intrinsic electrostatic interactions and fields because they are among the most concentrated electrolytic fluids with many charge carriers per unit volume. The strength of the intrinsic electric fields depends on cation–anion interaction, furthermore, this interaction is determined by the size and structure of cation and anion. The electric fields of [HMIm][X] ILs apparently decrease with increasing of anion size because of weakening the electrostatic interaction between ions. Moreover, for a symmetric anion, the intrinsic electric fields on its different subunits are partially canceled out due to the symmetry, so the net electric field on the whole anion is relatively small. For an asymmetric anion, such as [NTf₂], the intrinsic electric fields on its subunits are very different, so the net electric field on the whole anion is larger than the symmetric ones.^{34–36} Because the charge carriers of ILs are mobile via intrinsic electrostatic interactions and fields, they have very high conductivities.

3.2. Analytical Results of the Lubricating Greases.

FTIR spectra of the lubricating greases before and after irradiation are shown in Figure 2. The peaks at 3161 and 3122 cm^{-1} are due to the HCCH antisymmetric stretching and NC(H)N stretching on the imidazolium ring of LB106 and L-F106, respectively. The C–C band and C–N band on the imidazolium ring have the characteristic peaks at 1640 and 1572 cm^{-1} .^{37,38} The absorption peaks at both 1377 and 1470 cm^{-1} are assigned to the saturated alkyl group $-\text{CH}_3$ and $-\text{CH}_2-$. The band of B–F stretching vibration is at 1030 cm^{-1} . The

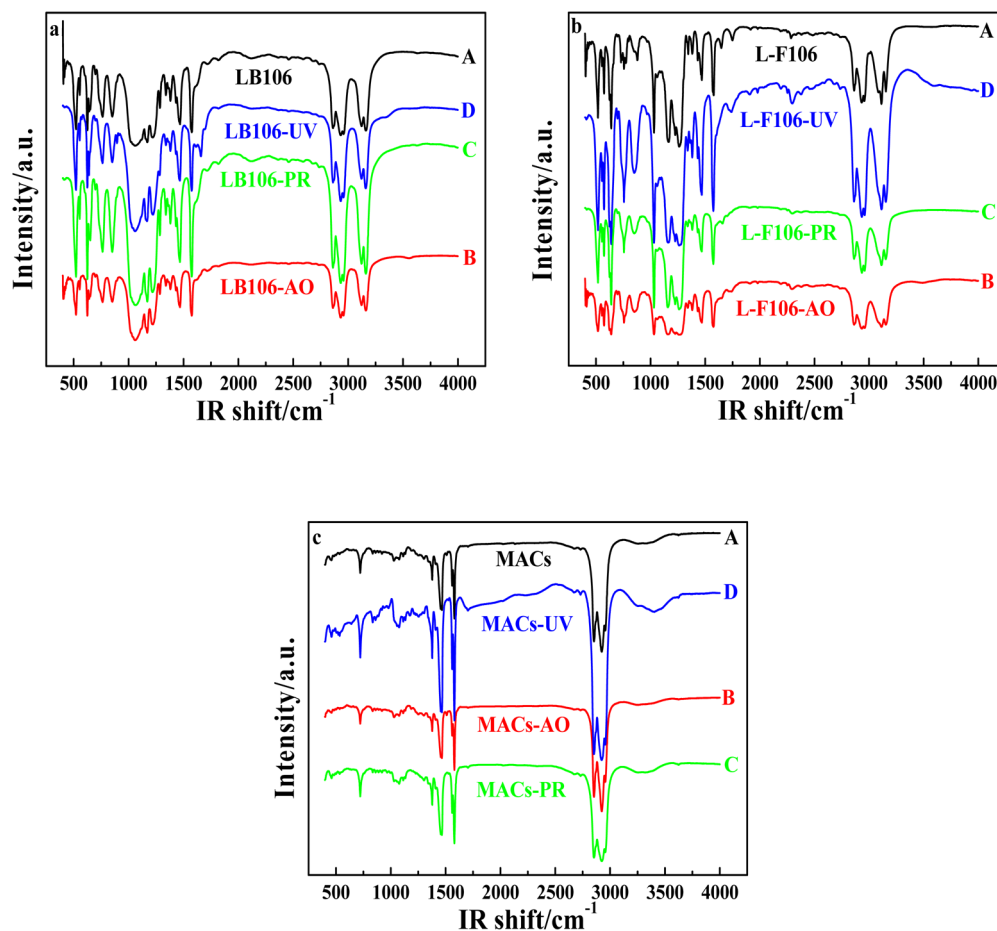


Figure 2. Fourier transform infrared analysis spectra of the lubricating greases before and after irradiation ((A) no irradiation, (B) AO, (C) PR, and (D) UV).

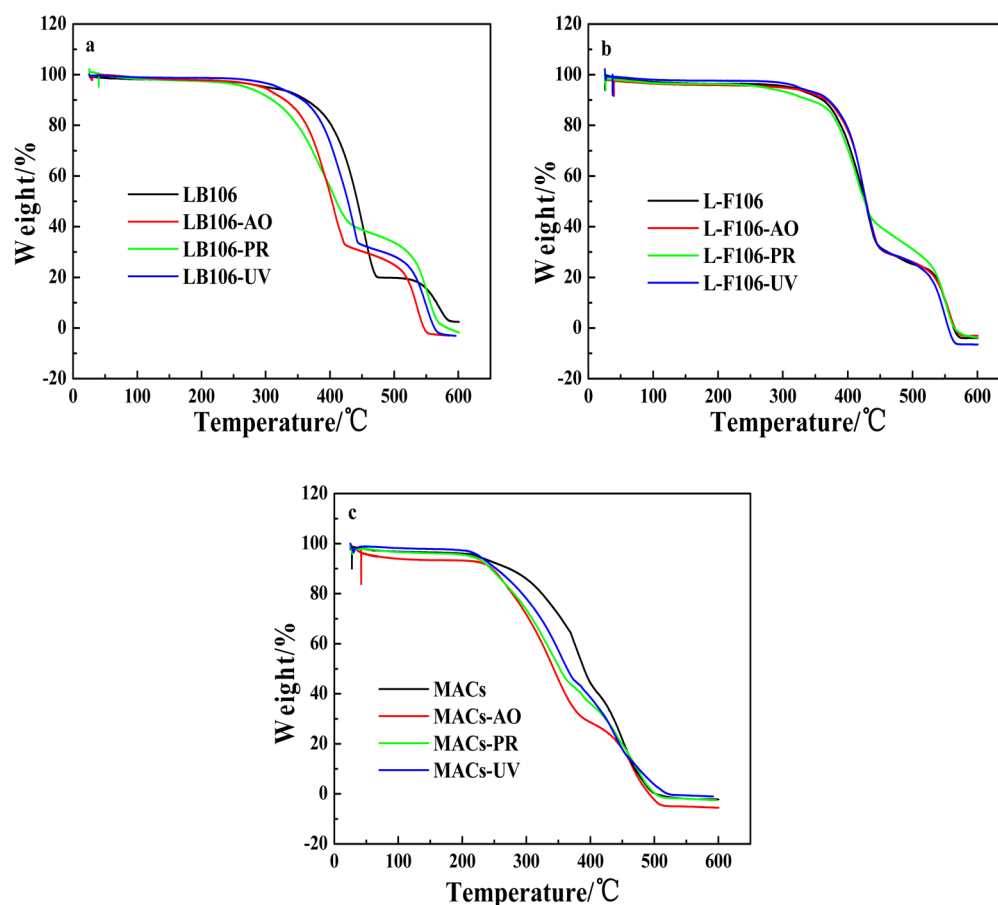


Figure 3. Thermogravimetric analysis curves of the lubricating greases before and after irradiation (black, no irradiation; red, AO; green, PR; and blue, UV).

Table 4. Change of Elemental Composition of the Lubricating Greases

sample	element					
	C	F	N	B	S	O
MACs	85.93	9.68				4.39
MACs-AO	95.27	0.89				3.84
MACs-PR	93.70	1.54				4.76
MACs-UV	95.91	0.17				3.92
LB106	50.50	31.56	4.55	12.43		0.96
LB106-AO	49.12	32.21	4.79	12.86		1.03
LB106-PR	64.78	15.79	1.62	13.05		4.76
LB106-UV	49.95	32.09	4.70	12.82		0.44
L-F106	41.14	37.70	4.39		6.22	10.54
L-F106-AO	42.66	31.99	6.30		5.83	13.22
L-F106-PR	42.28	30.28	6.02		9.05	12.37
L-F106-UV	44.09	30.17	4.82		9.82	11.10

bands of $-\text{SO}_2$ and $-\text{CF}_3$ on the NTf_2^- anions are at 1178 and 1269 cm^{-1} .^{39,40} The absorption bands in the range of 2950–2850 cm^{-1} are assigned to the C–H stretching of the alkyl chains on the MACs. The peaks in the range of 1575–1452 cm^{-1} are observed due to the CH_2 scissoring vibration.⁴¹ It can be shown that all the spectra are quite similar and no new peaks are detected from the lubricating greases after irradiation. Although no chemical reaction takes place during irradiation process, the destruction of alkyl chains on the ILs and MACs may have occurred.

TGA curves for the lubricating greases before and after irradiation are shown in Figure 3. It is noted in Figure 3a that the four TGA curves of LB106 grease nearly overlap at temperature up to 300 °C, and its decomposition before irradiation occurs at about 400 °C, whereas the decomposition after irradiation is in a slightly lower temperature range from 320 to 375 °C. This suggests that irradiation caused partial destruction of the LB106 molecules structure. The four TGA curves of L-F106 grease before and after irradiation nearly overlap in the testing temperature range from 50 to 600 °C in Figure 3b. The decomposition occurs at about 380 °C because the L-F106 grease has excellent thermal stability and high heat capacity, irradiation has almost no effect on its molecular structure. Figure 3c shows the four TGA curves of MACs grease before and after irradiation, the MACs grease after irradiation exhibits a significant change of decomposition temperature from 327 °C down to 252 °C, indicating that MACs has undergone serious structural damage during the irradiation process. Overall, TGA curves illustrate that PR and AO irradiation have a significant effect on the thermal stability of the lubricating greases due to the destruction of the molecular structure by irradiation. It is very interesting that L-F106 has higher decomposition temperature compared to the LB106 and MACs before and after irradiation because of its good anti-irradiation characteristics.

More direct evidence for the changes in chemical composition of the lubricating greases after irradiation has been obtained from SEM-EDS spectra which provide significant discrimination for chemical composition. Table 4

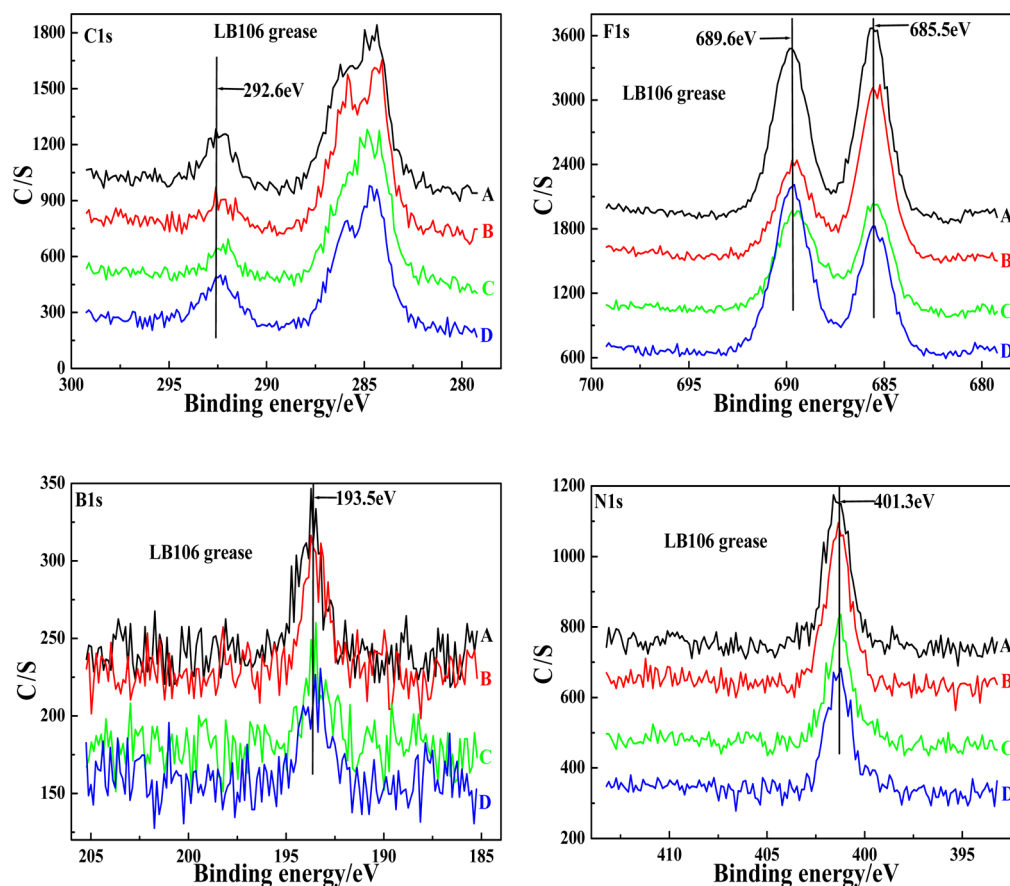


Figure 4. X-ray photoelectron spectra of the elements in the LB106 grease before and after irradiation ((A) no irradiation, (B) AO, (C) PR, and (D) UV).

shows the elemental composition of the lubricating greases before and after irradiation. Comparison of the changes in the elemental composition of MACs grease, the mass percentage of C and F elements have greatly changed after irradiation. The mass percentage of C element after irradiation increased by about 10%, while the mass percentage of F largely decreased from 9.68 wt % to 1.54 wt % (PR irradiation) and less than 1.0 wt % (AO and UV irradiations). This indicates that the MACs grease under irradiation environment took place severe decomposition. Observation the elemental mass percentage of LB106 grease before and after irradiation, the elemental percentage has only slight changes apart from the PR irradiation. The C elemental mass percentage increased from 50.50 wt % to 64.78 wt %, and the O percentage increased from 0.96 wt % to 4.76 wt %, but the F percentage decreased by 50% (from 31.56 wt % to 15.79 wt %) after PR irradiation. High-energy PR beam caused oxidation of LB106 grease. As can be shown in Table 4, the elemental mass percentage of L-F106 grease has also slightly changed after irradiation. The F percentage decreased by about 19%, while the C and O percentage increased slightly. It is very surprising that the N percentage largely increased after AO and PR irradiation, and the S percentage also significantly increased after PR and UV irradiations. It is possible that some weak bonds like F element of the ILs were broken and active elements like N and S were activated and reacted with other elements during the irradiation process. Although SEM-EDS has the advantages of being nondestructive for the sample, it only provides chemical composition of the sample.

To further explore the changes in the lubricating greases, we used XPS to clarify the chemical states of the sample's elements after irradiation. Figure 4 gives the XPS spectra of the LB106 grease before and after irradiation. XPS peaks of C 1s, F 1s, B 1s, and N 1s are observed in Figure 4. Two distinct C groups have been detected in the C 1s spectra: the lower binding energy range from 284.2 to 285.9 eV are assigned to CH₂ group and C–N bond in the cation of LB106 ILs;⁴² the higher binding energy appear at 292.6 eV, which could be attributed to the CF₂ group in PTFE.⁴³ The B 1s peaks at about 193.6 eV are assigned to BF₄ anion of LB106 ILs. XPS peaks of N 1s and F 1s were also obtained to further determine the type of compounds, the N 1s peak is located at 401.3 eV, which is identified as the C–N binding in the imidazolium ring of LB106 ILs, and the F 1s peaks appear at 685.5 and 689.6 eV, which correspond to BF₄ anion and CF₂, respectively.⁴⁴ For the LB106 grease after AO and PR irradiation, the high binding energy C 1s peaks had slightly shift to 291.96 eV, and the F 1s peaks shifted slightly to 685.2 and 698.4 eV, respectively.⁴⁵ The shift suggests that high-energy irradiation has caused the partial decomposition of the BF₄[−] anion and PTFE.

Figure 5 shows the XPS spectra of the L-F106 grease before and after irradiation including C 1s, F 1s, N 1s and S 1s. The C 1s peaks appear at the binding energy between 284.5 and 285.8 eV, which are assigned to the CH₂ groups of alkyl chains and C–N bonds of imidazolium rings. The C 1s peak at about 292.0 eV is attributed to the CF₂ group. The F 1s peaks with strong intensity at 688.3 eV are due to abundant CF₂ and CF₃ groups from the PTFE and the anion of LF106, respectively.

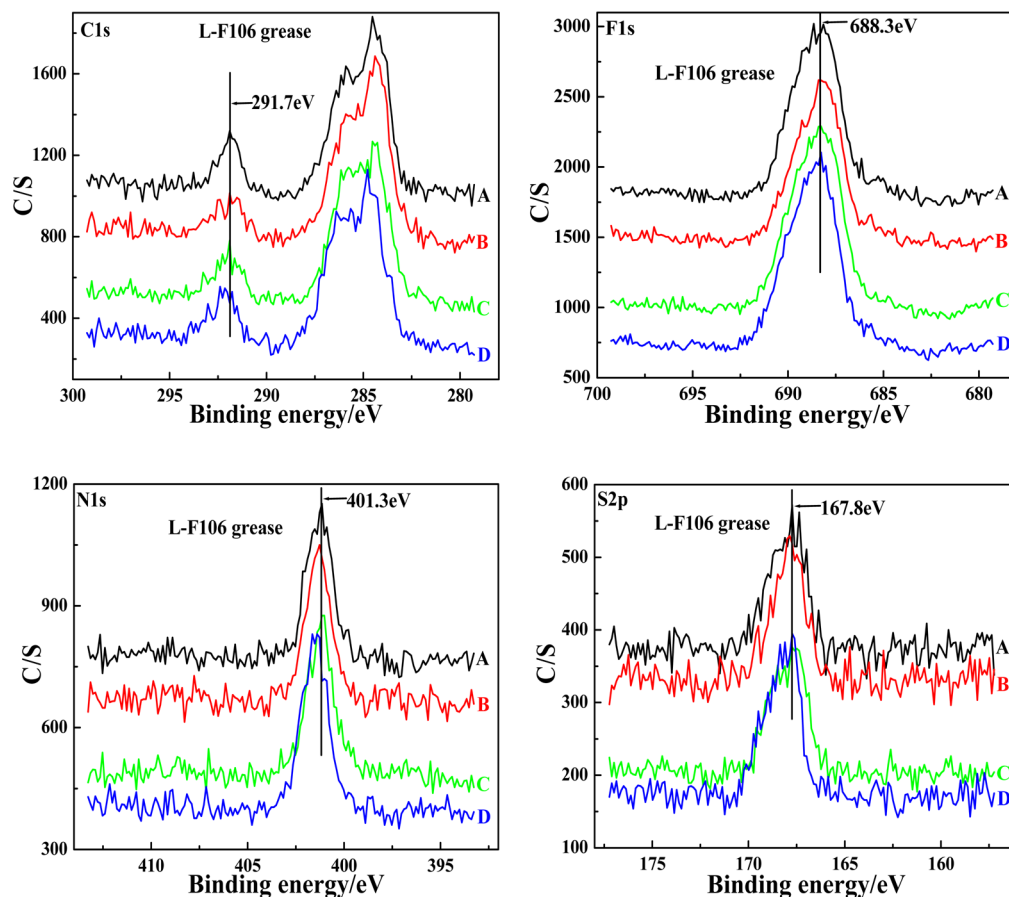


Figure 5. X-ray photoelectron spectra of the elements in the L-F106 grease before and after irradiation ((A) no irradiation, (B) AO, (C) PR, and (D) UV).

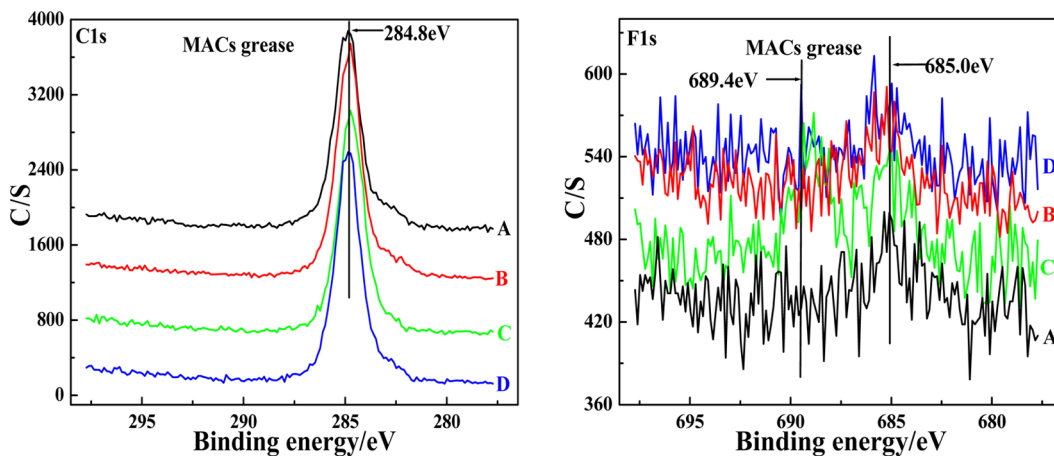


Figure 6. X-ray photoelectron spectra of the elements in the MACs grease before and after irradiation ((A) no irradiation, (B) AO, (C) PR, and (D) UV).

The N 1s peak at 401.3 eV is identified as the C–N binding in the imidazolium ring of LF106 ILs. The S 2p peak appears at 167.8 eV, which is assigned to the SO_2 group from the anion of LF106 ILs. Because the L-F106 grease has good anti-irradiation performance, its XPS spectra before and after irradiation had no obvious changes.

Figure 6 provides the XPS C 1s and F 1s spectra of the MACs grease. The peak of C 1s at 284.8 eV is identified as C in air. The CH_2 peaks of MACs grease do not clearly appear before and after irradiation, the possible reason is that the

intensity of C 1s peaks at 284.8 eV is so strong that other peaks are weakened and even disappear. The F 1s peaks of MACs grease with PR irradiation appear at 689.4 eV, which is attributed to CF_2 groups. This is because high-energy PR irradiation caused the decomposition of PTFE, and generated so abundant CF_2 groups that CF_2 peaks could be detected.

Combined with these experimental results before and after irradiation, the destructive effect of PR irradiation is the strongest than AO and UV irradiation, and UV irradiation occurs the weakest destructive effect. Atomic oxygen is the

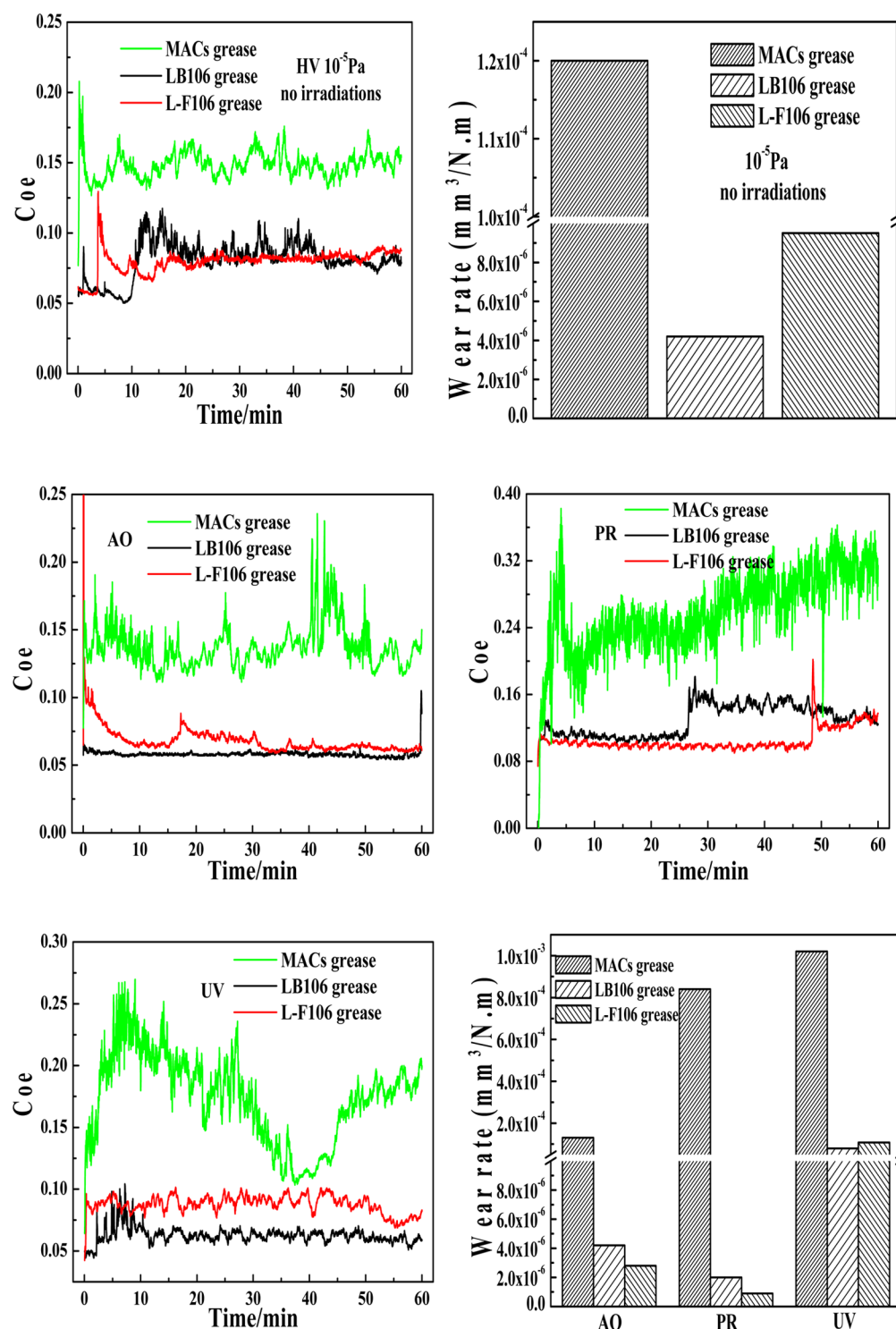


Figure 7. Friction coefficient and wear rate of the lubricating greases before and after irradiation.

major atmospheric constituent in low Earth orbit.^{46,47} If the lubricating greases were exposed to active atomic oxygen environment, the C atoms of the lubricating greases would be oxidized to CO and CO₂ into surrounding circumstances. Galactic cosmic rays spectrum are composed of 98% baryon component and 2% lepton component, and the baryon component consists of 87% protons and 13% ions.^{48,49} It is very significant topics about destructive mechanism of energetic protons under space environment. Heavy energetic protons bombard the surface of the samples, the kinetic energy and

positive charge of the incident protons can make the atoms in excited and ionized state. Moreover, the bombardment including elastic and inelastic collision are also involved. In an elastic collision, a portion of bombarding proton's energy are transmitted to an atom of the samples, and can cause the atom leaving from its lattice position as long as the imparted energy is so strong that the atom could be dislodged. The displaced atom will be ionized due to energy loss or displace other lattice atoms. Inelastic collision captures the incident protons and subsequent releases the protons at a lower energy level. The

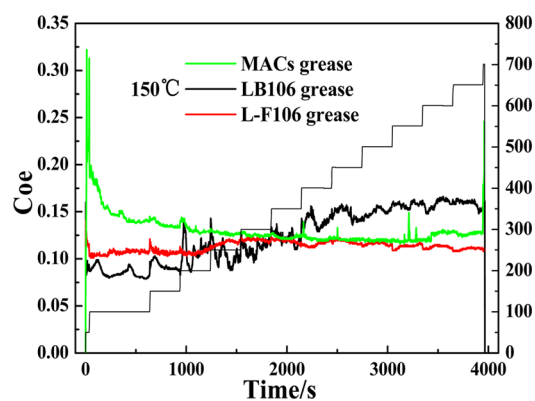


Figure 8. Extreme pressure property of the lubricating greases at 150 °C.

sample's atom is excited by the energy which is lost in this process, both the excited atom returns to the initial state and the kinetic energy of the incident protons is reduced by heat loss.^{50,51} According to the analysis of EDS and XPS, the structure of the lubricating greases occurred damage to a certain extent after PR irradiation because the energetic proton excited the C atom reaction with O atoms and induced the partial decomposition of the BF_4^- and NTf_2^- anions of ILs. Moreover, the destructive effect of charged particles for the MACs grease is much stronger than that of ILs greases because the highly polar ILs have high conductivity and heat capacity.^{52,53}

Figure 7 shows the friction curves and wear rate of the ILs greases and MACs grease before and after irradiation. The friction coefficients of ILs greases are always much smaller (<0.1) than that of MACs grease (~ 0.2) before and after irradiation. Surprisingly, the friction coefficients of the lubricating greases after AO and UV irradiation become smaller than before irradiation, but the friction coefficient occurred a slight rise after PR irradiation. The wear rate of the steel disc lubricated by the ILs greases ($\sim 1 \times 10^{-6} \text{ mm}^3 \text{ N}^{-1} \text{ m}^{-1}$) is about 2 orders of magnitude smaller than that of MACs grease ($\sim 1 \times 10^{-4} \text{ mm}^3 \text{ N}^{-1} \text{ m}^{-1}$) before and after irradiation. The wear rate of the steel disc under ILs lubrication with AO and PR irradiation is much smaller than that of the ILs greases before irradiation. It is very significant for the ILs greases after PR irradiation to reduce the degree of wear rate, while the wear rate increases to some extent after UV irradiation, since highly polar ILs have high conductivity and high heat capacity. Under

energetic irradiation, long alkyl chains of MACs and some weak C–F bonds of PTFE molecules were so severely damaged that the MACs showed poor lubrication. The alkyl chains and weak bonds of the ILs were partial decomposition and some atoms of ILs were activated by bombardment of high energy particles. These excited atoms could readily react with Fe atoms on the rubbing surfaces and generate a tribo-chemical reaction film to improve lubrication efficiency.

Figure 8 displays the extreme pressure properties of the lubricating grease at 150 °C. The ILs greases remain stable and are lower friction coefficient (~ 0.12) before applied load up to 700N, which is attributed to the high thermal stability and excellent tribological property of ILs grease. Figure 9 provides the tribological property of the lubricating greases under high temperature (200 °C) and high vacuum ($1 \times 10^{-5} \text{ Pa}$). The L-F106 grease has the smallest friction coefficient (0.06) and the lowest wear rate ($1.2 \times 10^{-4} \text{ mm}^3 \text{ N}^{-1} \text{ m}^{-1}$), followed by the LB106 grease (0.17 and $1.4 \times 10^{-2} \text{ mm}^3 \text{ N}^{-1} \text{ m}^{-1}$) and the MACs grease gives unstable and the maximum friction coefficient. The results confirm that ILs greases still possess good friction reducing and antiwear abilities in such a harsh environment, which depend on their high thermal stability and high heat capacity. Figure 10 gives the morphologies of the wear tracks under 200 °C and $1 \times 10^{-5} \text{ Pa}$ conditions. It can be observed that the worn surface lubricated by the L-F106 grease has small and narrow wear tracks, the worn surface lubricated by the LB106 grease appears significant plastic deformation, the worn surface with lubrication by MACs grease shows deep and wide wear tracks and large scars which were dominated by adhesive wear and fatigue wear.^{54,55} These results indicate that the ILs greases have better lubrication performance than the MACs grease under high temperature and high vacuum because ILs have low volatility and excellent thermal stability as well as high heat capacity.

To further explore the friction reducing and antiwear mechanism of the lubricating greases under simulated space conditions, we obtained the XPS spectra of the worn tracks to verify the tribo-chemical products. Figure 11 gives the XPS spectra of F 1s and Fe 2p on the worn tracks. XPS F 1s spectra at about 684.9 eV are attributed to fluoride including FeF_2 and FeF_3 .^{56,57} To further determine the type of generating compounds, XPS spectra of Fe 2p was detected at 711.3–711.4 eV, which are assigned to FeF_2 .^{58,59} The tribo-chemical reaction occurred on the rubbing surface to form a boundary

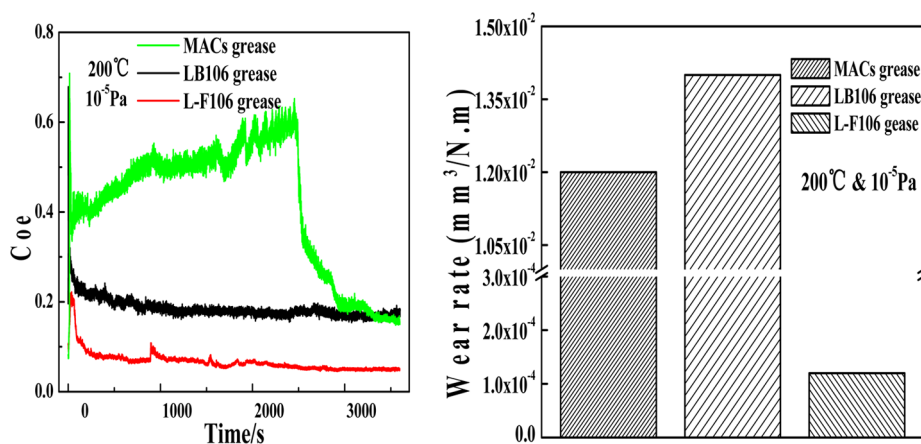


Figure 9. Tribological properties of the lubricating greases under high temperature and high vacuum.

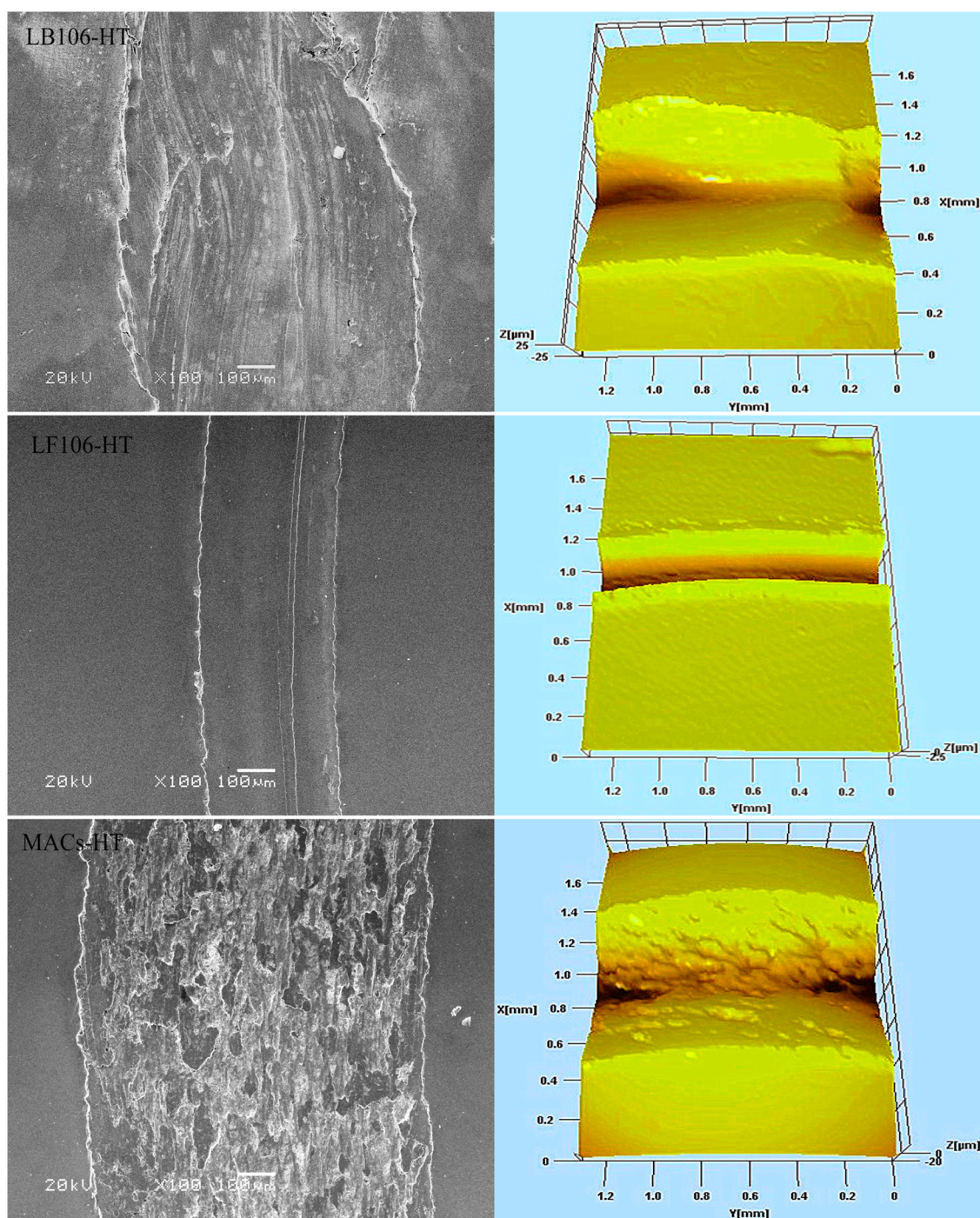


Figure 10. SEM and 3D images of the worn surfaces under high temperature and high vacuum.

protective film for improvement of friction reducing and antiwear properties.

Combined with experimental characterization and analysis of the lubricating greases before and after irradiation, it is confirmed that the ILs greases not only have strong anti-irradiation performance because of their physicochemical properties including good conductivity, excellent thermal stability, high heat capacity, and low volatility but also provide excellent tribological properties under space conditions because the abundant fluorine in ILs greases could generate a tribochemical reaction protective film to enhance tribological performance.

4. CONCLUSIONS

The physicochemical properties and tribological performance of high conductive ILs greases and MACs grease have been systematically studied under simulated space environment including high vacuum, high temperature and irradiation (ultraviolet, atomic oxygen and proton). The conclusions can be drawn from the characterization and analysis of the lubricating greases before and after tests as following:

- Alkyl imidazolium ILs greases have high conductivity because ILs exist strong intrinsic electric fields.
- Alkyl imidazolium ILs greases have stronger anti-irradiation capacity than MACs under simulated space

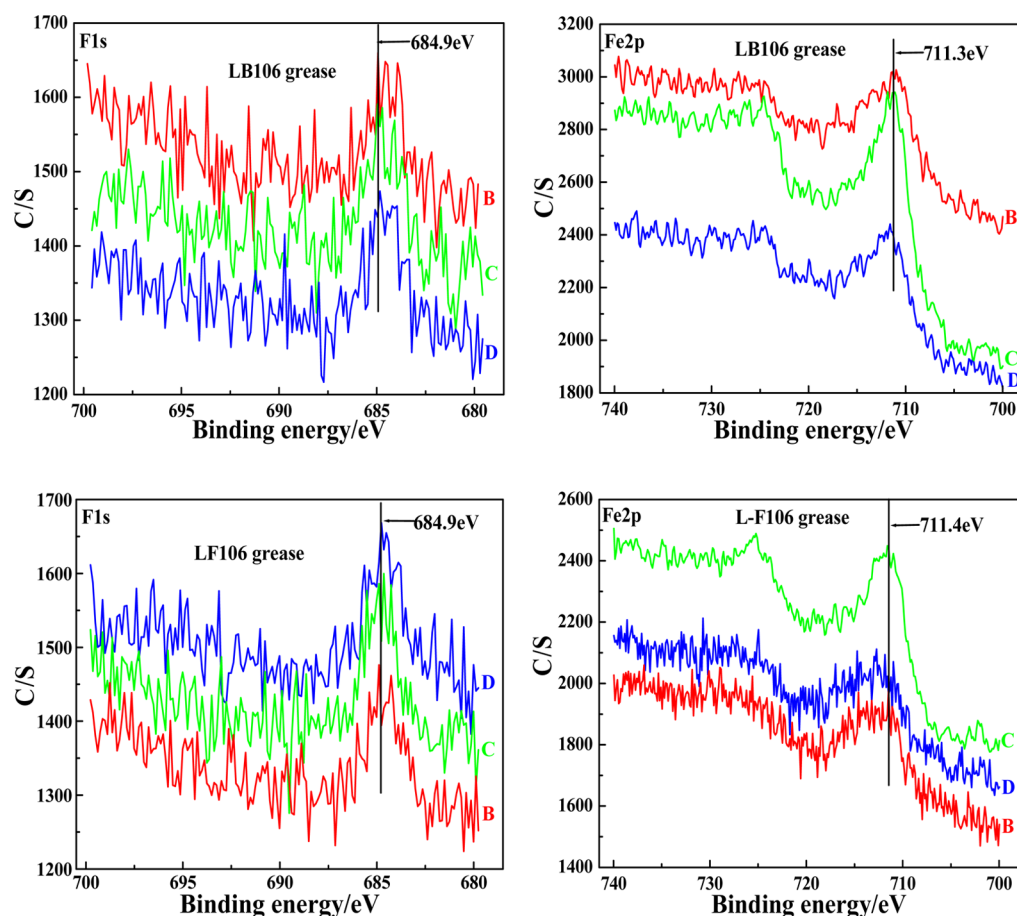


Figure 11. X-ray photoelectron spectra of the F and Fe elements on the wear surface ((B) AO, (C) PR, and (D) UV).

conditions because the ILs have the unique structure (high polar molecules via a combination of specific cations and anions) and physicochemical properties (good conductivity, high thermal stability and heat capacity, as well as low volatility).

- (c) Alkyl imidazolium IL greases have the excellent friction reducing and antiwear performance and extreme pressure property under high temperature and high vacuum.
- (d) After irradiation, alkyl imidazolium IL greases show much lower friction coefficient and smaller wear rate than before irradiation since the increasing reactive groups through irradiation are easily adsorbed on the worn surfaces to form physical adsorption film and the tribo-chemical reaction film could be also formed during sliding process. Therefore, the excellent tribological performances are obtained by adsorption film and reaction film synergies.

AUTHOR INFORMATION

Corresponding Author

*E-mail: lpwang@licp.cas.cn. Tel: +86-0931-4968080.

Notes

The authors declare no competing financial interest.

ACKNOWLEDGMENTS

The authors are grateful for financial support from the National Natural Science Foundation of China (11172300 and 51322508).

REFERENCES

- (1) Takano, A. Tribology-Related Space Mechanism Anomalies and the Newly Constructed High-Vacuum Mechanism Test Facilities in NASDA. *Tribol. Int.* **1999**, *32*, 661–671.
- (2) Jones, W. R., Jr.; Jansen, M. J. *Space Tribology*; NASA/TM–2000–209924 ; National Aeronautics and Space Administration: Washington, D.C..
- (3) Fusaro, R. L. *Preventing Spacecraft Failure due to Tribological Problems*; NASA/TM–2001–210806 ; National Aeronautics and Space Administration: Washington, D.C..
- (4) Zaretsky, E. V. Liquid Lubrication in Space. *Tribol. Int.* **1990**, *23*, 75–93.
- (5) Durfane, K. F.; Kannel, J. W.; Lowry, J. A. *Lubricant Selection Manual*. NASA/CR–1991–18436.
- (6) Brostow, W.; Kovačević, V.; Vrsaljko, D.; Whitworth, J. Tribology of Polymers and Polymer-Based Composites. *J. Mater. Ed.* **2010**, *32*, 273–290.
- (7) Suzuki, A.; Shinka, Y.; Masuko, M. Tribological Characteristics of Imidazolium-Based Room Temperature Ionic Liquids under High Vacuum. *Tribol. Lett.* **2007**, *27*, 307–313.
- (8) Jones, W. R., Jr.; Shogrin, B. A.; Jansen, M. J. Research on Liquid Lubricants for Space Mechanisms. *J. Synth. Lubr.* **2000**, *17*, 109–122.
- (9) Masuko, M.; Jones, W. R., Jr.; Helmick, L. S. Tribological Characteristics of Perfluoropolyether Liquid Lubricants under Sliding Conditions in High Vacuum. *J. Synth. Lubr.* **1994**, *11*, 111–119.
- (10) Srour, J. R.; McGarrity, J. M. Radiation Effects on Microelectronics in Space. *Proc. IEEE* **1988**, *76*, 1443–1469.
- (11) Grossman, E.; Gouzman, I. Space Environment Effects on Polymers in Low Earth Orbit. *Nucl. Instrum. Methods Phys. Res., Sect. B* **2003**, *208*, 48–57.
- (12) Liu, X.; Wang, L.; Xue, Q. DLC-based Solid–Liquid Synergetic Lubricating Coatings for Improving Tribological Behavior of Boundary

Lubricated Surfaces under High Vacuum Condition. *Wear* **2011**, *271*, 889–898.

(13) Zhao, X.; Shen, Z.; Xing, Y.; Ma, S. An Experimental Study of Low Earth Orbit Atomic Oxygen and Ultraviolet Radiation Effects on a Spacecraft Material-Polytetrafluoroethylene. *Polym. Degrad. Stab.* **2005**, *88*, 275–285.

(14) Rosenzweig, W.; Smits, F. M.; Brown, W. L. Energy Dependence of Proton Irradiation Damage in Silicon. *J. Appl. Phys.* **1964**, *35*, 2707–2711.

(15) Srour, J. R.; Hartmann, R. A.; Kitazaki, K. S. Permanent Damage Produced by Single Proton Interactions in Silicon Devices. *IEEE Trans. Nucl. Sci.* **1986**, *33*, 1597–1604.

(16) Freire, M. G.; Carvalho, P. J.; Fernandes, A. M.; Marrucho, I. M.; Queimada, A. J.; Coutinho, J. A. P. Surface Tensions of Imidazolium Based Ionic Liquids: Anion, Cation, Temperature and Water Effect. *J. Colloid Interface Sci.* **2007**, *314*, 621–630.

(17) Wang, J.; Wang, H.; Zhang, S.; Zhang, H.; Zhao, Y. Conductivities, Volumes, Fluorescence, and Aggregation Behavior of Ionic Liquids [C_nmim][BF₄] and [C_nmim]Br (n = 4, 6, 8, 10, 12) in Aqueous Solutions. *J. Phys. Chem. B* **2007**, *111*, 6181–6188.

(18) Lu, W.; Fadeev, A. G.; Qi, B.; Smela, E.; Mattes, B. R.; Ding, J.; Spinks, G. M.; Mazurkiewicz, J.; Zhou, D.; Wallace, G. G.; Macfarlane, D. R.; Forsyth, S. A.; Forsyth, M. Use of Ionic Liquids for π -Conjugated Polymer Electrochemical Devices. *Science* **2002**, *297*, 983–987.

(19) Somers, A. E.; Khemchandani, B.; Howlett, P. C.; Sun, J.; MacFarlane, D. R.; Forsyth, M. Ionic Liquids as Antiwear Additives in Base Oils: Influence of Structure on Miscibility and Antiwear Performance for Steel on Aluminum. *ACS Appl. Mater. Interfaces* **2013**, *5*, 11544–11553.

(20) Ye, C.; Liu, W.; Chen, Y.; Yu, L. Room-Temperature ILs: A Novel Versatile Lubricant. *Chem. Commun.* **2001**, *21*, 2244–2245.

(21) Yao, M.; Fan, M.; Liang, Y.; Zhou, F.; Xia, Y. Imidazolium Hexafluorophosphate ILs as High Temperature Lubricants for Steel-Steel Contacts. *Wear* **2010**, *268*, 67–71.

(22) Battez, A. H.; González, R.; Viesca, J. L.; Blanco, D.; Asedegbega, E.; Osorio, A. Tribological Behaviour of Two Imidazolium ILs as Lubricant Additives for Steel/Steel Contacts. *Wear* **2009**, *266*, 1224–1228.

(23) Jimenez, A. E.; Bermudez, M. D. Imidazolium ILs as Additives of the Synthetic Ester Propylene Glycol Dioleate in Aluminium-Steel Lubrication. *Wear* **2008**, *265*, 787–798.

(24) Fan, X.; Xia, Y.; Wang, L.; Pu, J.; Chen, T.; Zhang, H. Study of the Conductivity and Tribological Performance of Ionic Liquid and Lithium Greases. *Tribol. Lett.* **2014**, *53*, 281–291.

(25) Jiménez, A. E.; Bermúdez, M. D. ILs as Lubricants for Steel-Aluminum Contacts at Low and Elevated Temperatures. *Tribol. Lett.* **2006**, *26*, 53–60.

(26) Xia, Y.; Sasaki, S.; Murakami, T.; Nakano, M.; Shi, L.; Wang, H. Ionic Liquid Lubrication of Electrodeposited Nickel-Si₃N₄ Composite Coatings. *Wear* **2007**, *262*, 765–771.

(27) Feng, X.; Xia, Y. Tribological Properties of Ti-doped DLC Coatings under ILs Lubricated Conditions. *Appl. Surf. Sci.* **2012**, *258*, 2433–2438.

(28) Cammarata, L.; Kazarian, S.; Salter, P.; Welton, T. Molecules States of Water in Room Temperature ILs. *Phys. Chem. Chem. Phys.* **2001**, *3*, 5192–5200.

(29) Bonhôte, P.; Dias, A. P.; Papageorgiou, N.; Kalyanasundaram, K.; Grätzel, M. Hydrophobic, Highly Conductive Ambient-Temperature Molten Salts. *Inorg. Chem.* **1996**, *35*, 1168–1178.

(30) Welton, T. Room-temperature Ionic Liquids. Solvents for Synthesis and Catalysis. *Chem. Rev.* **1999**, *99*, 2071–2083.

(31) Ji, L.; Li, H.; Zhao, F.; Quan, W.; Chen, J.; Zhou, H. Atomic Oxygen Resistant Behaviors of Mo/Diamond-like Carbon Nanocomposite Lubricating Films. *Appl. Surf. Sci.* **2009**, *255*, 4180–4184.

(32) Liu, Z. Effect of Component in Grease on Electric Property of Grease. *Petroleum Prod. Appl. Res.* **2000**, *18*, 12–15.

(33) Wang, Z.; Xia, Y.; Liu, Z. Conductive Lubricating Grease Synthesized Using the Ionic Liquid. *Tribol. Lett.* **2012**, *46*, 33–42.

(34) Zhang, S.; Rui, S.; Ma, X.; Lu, L.; He, Y.; Zhang, X.; Wang, Y.; Deng, Y. Intrinsic Electric Fields in Ionic Liquids Determined by Vibrational Stark Effect Spectroscopy and molecules Dynamics Simulation. *J. Eur. Chem.* **2012**, *18*, 11904–11908.

(35) Hapiot, P.; Lagrost, C. Electrochemical Reactivity in Room-Temperature Ionic Liquids. *Chem. Rev.* **2008**, *108*, 2238–2264.

(36) Taniki, R.; Matsumoto, K.; Hagiwara, R. Trialkylsulfonium Fluorohydrogenate Giving the Highest Conductivity in Room Temperature Ionic Liquids. *Electrochem. Solid. St.* **2012**, *15*, 13–15.

(37) Heimer, N. E.; Del Sesto, R. E.; Meng, Z. Z.; Wilkes, J. S.; Carper, W. R. Vibrational Spectra of Imidazolium Tetrafluoroborate Ionic Liquids. *J. Mol. Liq.* **2006**, *124*, 84–95.

(38) Dieter, K. M.; Dymek, C. J.; Heimer, N. E.; Rovang, J. W.; Wilkes, J. S. Ionic Structure and Interactions in 1-Methyl-3-Ethylimidazolium Chloride-Aluminum Chloride Molten Salts. *J. Am. Chem. Soc.* **1988**, *110*, 2722–2726.

(39) Seki, T.; Grunwaldt, J. D.; Baiker, A. In Situ Attenuated Total Reflection Infrared Spectroscopy of Imidazolium-Based Room-Temperature Ionic Liquids under “Supercritical” CO₂. *J. Phys. Chem. B* **2009**, *113*, 114–122.

(40) Xu, A.; Wang, J.; Wang, H. Effects of Anionic Structure and Lithium Salts Addition on the Dissolution of Cellulose in 1-Butyl-3-Methylimidazolium-Based Ionic Liquid Solvent Systems. *Green. Chem.* **2010**, *12*, 268–275.

(41) Shi, F.; Deng, Y. Abnormal FT-IR and FTRaman Spectra of Ionic Liquids Confined in Nano-porous Silica Gel. *Spectrochim. Acta, Part A* **2005**, *62*, 239–244.

(42) Ren, S.; Yang, S.; Zhao, Y.; Yu, T.; Xiao, X. Preparation and Characterization of an Ultrahydrophobic Surface Based on a Stearic Acid Self-Assembled Monolayer over Polyethyleneimine Thin Films. *Surf. Sci.* **2003**, *546*, 64–74.

(43) Sanders, J. H.; Cutler, J. N.; John, G. Characterization of Surface Layers on M-50 Steel Exposed to Perfluoropolyalkyethers at Elevated Temperatures. *Appl. Surf. Sci.* **1998**, *135*, 169–177.

(44) Liu, X.; Pu, J.; Wang, L.; Xue, Q. Novel DLC/Ionic Liquid/Graphene Nanocomposite Coatings towards High-Vacuum Related Space Applications. *J. Mater. Chem. A* **2013**, *1*, 3797–3809.

(45) Mu, Z.; Zhou, F.; Zhang, S.; Liang, Y.; Liu, W. Effect of the Functional Groups in Ionic Liquid Molecules on the Friction and Wear Behavior of Aluminum Alloy in Lubricated Aluminum-on-Steel Contact. *Tribol. Int.* **2005**, *38*, 725–731.

(46) Rao, J.; Lawson, K. J.; Nicholls, J. R. The Characterisation of E-beam Evaporated and Magnetron Sputtered Carbon Films Fabricated for Atomic Oxygen Sensors. *Surf. Coat. Technol.* **2005**, *197*, 154–160.

(47) Tagawa, M.; Muromoto, M.; Hachiue, S.; Yokota, K.; Ohmae, N.; Matsumoto, K.; Suzuki, M. Hyperthermal Atomic Oxygen Interaction with MoS₂ Lubricants and Relevance to Space Environmental Effects in Low Earth Orbit-Effects on Friction Coefficient and Wear-Life. *Tribol. Lett.* **2005**, *18*, 437–443.

(48) Petersen, E. L. Soft Errors due to Protons in the Radiation Belt. *IEEE Trans. Nucl. Sci.* **1981**, *28*, 3981–3986.

(49) Burke, E. A. Energy Dependence of Proton-Induced Displacement Damage in Silicon. *IEEE Trans. Nucl. Sci.* **1986**, *33*, 1276–1281.

(50) Benton, E. R.; Benton, E. V. Space Radiation Dosimetry in Low-Earth Orbit and Beyond. *Nucl. Instrum. Methods Phys. Res., Sect. B* **2001**, *184*, 255–294.

(51) Van Lint, V. A. J.; Flanagan, T. M.; Leadon, R. E.; Naber, J. A.; Rogers, V. C. *Mechanisms of Radiation Effects in Electronic Materials* Wiley. New York, 1980.

(52) Wilkes, J. S. A Short History of Ionic Liquids-from Molten Salts to Neoteric Solvents. *Green. Chem.* **2002**, *4*, 73–80.

(53) Yang, J.; Liu, Y.; Ye, Z.; Yang, D.; He, S. The Effect of Plasma Nitriding on the Tribology of Perfluoropolyether Grease-Lubricated 2Cr13 Steel Couples in Vacuum. *Tribol. Lett.* **2010**, *40*, 139–147.

(54) Myshkin, N. K.; Petrokovets, M. I.; Kovalev, A. V. Tribology of Polymers: Adhesion, Friction, Wear and Mass Transfer. *Tribol. Int.* **2005**, *38*, 910–921.

(55) Brostow, W.; Deborde, J. L.; Jaklewicz, M.; Olszynski, P. Tribology with Emphasis on Polymers: Friction, Scratch Resistance and Wear. *J. Mater. Ed.* **2003**, *25*, 119–132.

(56) Cai, M.; Liang, Y.; Yao, M.; Xia, Y.; Zhou, F.; Liu, W. Tribological Properties of Novel Imidazolium Ionic Liquids Bearing Benzotriazole Group as the Antiwear/Anticorrosion Additive in Poly(ethylene glycol) and Polyurea Grease for Steel/Steel Contacts. *ACS Appl. Mater. Interface* **2010**, *2*, 870–876.

(57) Fan, M.; Song, Z.; Liang, Y.; Zhou, F.; Liu, W. In Situ Formed Ionic Liquids in Synthetic Esters for Significantly Improved Lubrication. *ACS Appl. Mater. Interfaces* **2012**, *4*, 6683–6689.

(58) Phillips, B. S.; John, G.; Zabinski, J. S. Surface Chemistry of Fluorine Containing Ionic Liquids on Steel Substrates at Elevated Temperature Using Mössbauer Spectroscopy. *Tribol. Lett.* **2007**, *26*, 85–91.

(59) NIST X-ray Photoelectron Spectroscopy Database, version 4.1; National Institute of Standards and Technology: Gaithersburg, MD, 2012. Accessed on March 26, 2013. <http://srdata.nist.gov/xps/>.